Insect Biochemistry and Molecular Biology 118 (2020) 103311

Contents lists available at ScienceDirect

Insect Biochemistry and Molecular Biology

journal homepage: www.elsevier.com/locate/ibmb

Nix is a male-determining factor in the Asian tiger mosquito *Aedes albopictus*

Peiwen Liu[a,1], Binbin Jin[a,1], Xiaocong Li[a,1], Yijie Zhao[a], Jinbao Gu[a], James K. Biedler[b], Zhijian Jake Tu[b,**], Xiao-Guang Chen[a,*]

[a] Department of Pathogen Biology, Guangdong Provincial Key Laboratory of Tropical Disease Research, School of Public Health, Southern Medical University, Guangzhou, Guangdong, 510515, China

[b] Department of Biochemistry and the Fralin Life Science Institute, Virginia Tech, Blacksburg, VA, 24061, USA

ARTICLE INFO

Keywords:
M-factor
Sex-determination
CRSPR-Cas9
Feminized

ABSTRACT

The initial signal that governs sex determination is highly variable among insects. A homolog of *Nix*, the male-determining factor in *Aedes aegypti*, was previously found in the Asian tiger mosquito *Ae. albopictus*. Here we show that the *Ae. albopictus Nix* (*AalNix*) is more complex in gene structure and splice isoforms than its *Ae. aegypti* homolog (*AaeNix*). *AalNix* shows a similar transcription profile compared to *AaeNix*. CRISPR/Cas9-mediated knockouts of *AalNix in vivo* and in the *Ae. albopictus* C6/36 cells lead to a shift of *dsx* and *fru* splicing towards the female isoforms. G_0 knockout males showed feminization and deformities including feminized antennae, absence or partial absence of gonocoxites, gonostyli, testes and accessory glands, and the formation of ovaries. Despite ~70 MY of divergence, *Nix* functions as a conserved male-determining factor in the two most important arboviral vectors, namely *Ae. aegypti* and *Ae. albopictus*.

1. Introduction

Insects employ diverse primary signals to initiate a cascade of events that lead to sex-determination (Biedler and Tu, 2016; Bopp et al., 2014; Gempe and Beye, 2011; Sanchez, 2008; Schutt and Nothiger, 2000). In the fruit fly *Drosophila melanogaster*, the presence of two X chromosomes (XX) activates the expression of a splicing factor Sex-lethal (*Sxl*) which triggers a series of events leading to female-specific splicing of *dsx* and *fru* (Salz and Erickson, 2010). In the silkworm *Bombyx mori*, a W-linked Piwi-interacting RNA *Fem* is the primary signal responsible for female sex determination (Kiuchi et al., 2014). Sex determination in the honeybee *Apis mellifera* is governed by heterozygosity of the complementary sex determiner (*csd*) gene (Hasselmann et al., 2008). At the bottom of the sex-determination cascade, sex-specific splicing of the primary transcripts of two conserved genes, *doublesex* (*dsx*) and *fruitless* (*fru*), results in sex-specific isoforms of the DSX and FRU proteins that program sexual differentiation. Thus, diverse primary signals are transduced to conserved and sex-specific regulatory proteins to achieve sex-determination in insects (Bachtrog et al., 2014; Verhulst and van de Zande, 2015).

In a number of dipteran insects including mosquitoes and non-Drosophila flies, the primary signal of sex-determination is a dominant male determining factor (M factor) that resides either on the Y chromosome or the male-determining locus of a homomorphic sex-determining chromosome (Criscione et al., 2016; Gilchrist and Haldane, 1947; Hall et al., 2015a; Krzywinska et al., 2016; Marin and Baker, 1998; McClelland, 1962; Sharma et al., 2017). In the yellow fever and dengue fever mosquito, *Aedes aegypti,* a predicted RNA-binding protein encoded by the M factor gene *Nix* is both required and sufficient to initiate male development, and it confers male-specific splicing of *doublesex* and *fruitless* (Hall et al., 2015a). In two malaria mosquito species, *Anopheles stephensi and Anopheles gambiae*, Y chromosome genes that encode two apparently un-related 56 amino acid long proteins Guy1 and Yob/gYG2, appear to be the M factors, respectively (Criscione et al., 2013, 2016; Krzywinska et al., 2016). In the house fly *Musca domestica*, a male determiner (*Mdmd*) that encodes a paralog of a generic splicing factor is the M factor (Sharma et al., 2017).

We are interested in studying the evolution of *Nix* in related Aedes mosquitoes and the potential applications of genetic manipulations of the sex-determination pathway to reduce the number of biting and egg-laying female mosquitoes. Sexual dimorphism could be explored for the control of mosquito-borne infectious diseases because only females bite

* Corresponding author. Department of Pathogen Biology, School of Public Health, Southern Medical University, No.1023 South Shatai Road, Baiyun District, Guangzhou, Guangdong, 510515, China.

** Corresponding author. Department of Biochemistry, 303 Fralin, Virginia Tech, Blacksburg, VA, 24061, USA.

E-mail addresses: jaketu@vt.edu (Z.J. Tu), xgchen2001@hotmail.com (X.-G. Chen).

[1] These authors contributed equally to this work.

https://doi.org/10.1016/j.ibmb.2019.103311
Received 30 June 2019; Received in revised form 26 December 2019; Accepted 27 December 2019
Available online 31 December 2019

a vertebrate host and transmit disease-causing pathogens (Adelman and Tu, 2016; Biedler and Tu, 2016; Papathanos et al., 2009; Wise de Valdez et al., 2011). A homolog of the *Ae. aegypti Nix* (*AaeNix*) has been previously reported in the Asian tiger mosquito, *Aedes albopictus* (Hall et al., 2015a), a notorious invasive species that could transmit dengue and Zika viruses. The full-length *Ae. albopictus Nix* (*AalNix*) gene was recently reported in the genome assembly of the C6/36 cell line which was apparently established from male *Ae. albopictus* cells (Miller et al., 2018), and the Rimini strain of *Ae. albopictus* (Gomulski et al., 2018). However, functional analysis and detailed molecular characterization of the *Ae. albopictus Nix* gene have not been performed.

In the present study, we have demonstrated male specificity of *AalNix* in laboratory and field-collected *Ae. albopictus*, and identified an unexpected complexity in the number of isoforms of *AalNix* transcripts. The developmental expression profiles show that *Nix* expression in *Ae. albopictus* is similar to that in *Ae. aegypti* with the exception of a later start during the embryonic stage. Disruption of *Nix* with CRISPR/Cas9 shifted splicing of *dsx* and *fru* towards the female isoforms in both C6/36 cells and male mosquitoes. Furthermore, feminization and deformities were observed in nix-knockout male mosquitoes. These data support the conclusion that *Nix* is a conserved M factor in both *Ae. aegypti* and *Ae. albopictus*, and genetic manipulation of *Nix* may be explored to control these two most important arboviral vectors.

2. Materials and methods

2.1. Mosquitoes and cell lines

The *Ae. albopictus* Foshan strain (Foshan Guangdong Province, China) was established in the laboratory in 1981 and reared in 30-cm cube nylon cages in the insectary at 28 ± 1 °C with 70%–80% humidity and a 12:12 h (light: dark) light cycles. Larvae were fed with finely ground fish food, mixed 1:1 with yeast powder., and adults were fed with 10% glucose solution after emergence and mated freely. Female adults were blood feed with defibrinated sheep blood 3 days post-emergence for egg production. C6/36 (ATCC CRL-1660) was maintained at 28 °C in Roswell Park Memorial Institute (RPMI) 1640 medium (Gibco, Life Technology, China) with 10% fetal bovine serum (Gibco, Life Technology, Australia).

2.2. 5′ and 3′ rapid amplification of cDNA ends (RACE)

Total RNA was extracted from about 200 embryos between 24 and 48 h after oviposition, 15 male pupae, 15 male adults, and about 1×10^6 C6/36 cells with TRIzol® Reagent (Life Technologies, Carlsbad CA, USA) following manufacturer's instructions. The RNA quantity and quality was determined using a NanoDrop 2000 Spectrophotometer (Thermo Scientific) and by gel electrophoresis with a 1.5% agarose gel. According to the user manual of FirstChoice RLM-RACE Kit (Life Technologies, Carlsbad CA, USA), NixGSPF1 and NixGSPF2 primers were designed (Supplementary Table S1). The 5′ and 3′ RACE products were purified from 1% agarose gels with the GeneJET Gel Extraction Kit (Thermo Fisher Scientific, Carlsbad CA, USA), cloned into pJET1.2/blunt Cloning Vector (Thermo Fisher Scientific, Carlsbad CA, USA) and sequenced.

2.3. Qualitative and quantitative RT-PCR

For *Nix* male-specificity validation, genomic DNA was extracted from male and female adults, and C6/36 cells using MiniBEST Universal Genomic DNA Extraction Kit (Takara-Bio, Shiga, Japan). For *AalNix*, *Ae. albopictus doublesex* (*Aaldsx*) and *Ae. albopictus fruitless (Aalfru)* transcription analysis, total RNA was extracted from C6/36 cells and mosquitoes using the TRIzol® Reagent (Life Technologies, Carlsbad CA, USA). The RNA quantity and quality was determined using a NanoDrop 2000 Spectrophotometer and by gel electrophoresis with a 1.5% agarose gel. 10 μg Total RNA was digested using TURBO DNA-free™ Kit (Life Technologies, Carlsbad CA, USA) to remove genomic DNA following the manufacturer's protocol. cDNA was synthesized with GoScript Reverse Transcription System (Promega Corporation, Madison WI, USA) in a 20 μl reaction mixture containing 2 μg total RNA. PCR was carried out using Maxima Hot Start Green PCR Master Mix (2 ×) (Thermo Fisher Scientific, Waltham, MA, USA) and *Ae. albopictus* ribosomal protein 7 (*AalRpS7*) was used as an internal control.

For quantitative mRNA analysis, quantitative PCR (qPCR) was performed using SuperReal PreMix Plus kit (SYBR Green) (Tiangen Biotech Co., Ltd., Beijing, China) and an ABI7500 system according to the manufacturer's protocol. Each sample was assessed in triplicate and normalized with *AalRpS7* mRNA. The qPCR results were analyzed using the $2^{-\Delta\Delta CT}$ method. All the primers for qualitative and quantitative PCR were shown in Table S1.

2.4. Design and preparation of sgRNA for CRISPR/Cas9

The exon 1 of *Nix* was used to design and determine optimum candidate sgRNAs by the CRISPR Design Tool website (http://www.rgenome.net/cas-designer/) (Park et al., 2015). According to the core based off-target analysis, top two, sgRNA1 and sgRNA2 were selected, which target *AalNix* at positions 315 and 466 respectively (Supplementary Table S2). A guanine was added to the first base of the sgRNA to improve efficiency of host U6 promoter transcription. For knockout of *AalNix* in C6/36 cells, sgRNA1-2 synthesized template oligos (Supplementary Table S2) were cloned into the Drosophila CRISPR vector pAc-sgRNA-Cas9, which was a gift from Ji-Long Liu (Addgene plasmid 49330) (Bassett et al., 2014). Vectors were confirmed by direct sequencing. The CRISPR vector contains two main components. One is a human codon-optimized N-terminal FLAG-tagged Streptococcus pyogenes Cas9 enzyme linked to a puromycin resistance gene by a T2A polyprotein self-cleavage site (Kim et al., 2011; Varjak et al., 2017). The other is an sgRNA scaffold downstream of the Drosophila U6 promoter which is transcribed by Pol III RNA polymerase. For CRISPR/Cas9-mediated knock-in in C6/36 cells, the donor plasmid was constructed by insertion of T2A-Puro into pIEXBac1-DsRed between *Bam*HI and *Hind*III. For KO of *AalNix in vivo*, sgRNA1/2 were used as templates for *in vitro* transcription following PCR with a universal oligo (Supplementary Table S2). T7-driven sgRNA was transcribed *in vitro* using the T7 RiboMAX Express Large Scale RNA Production System (Promega Corporation, Madison WI, USA) following the manufacturer's protocol.

2.5. Nix knockout with CRISPR/Cas9 in C6/36 cells

One day before transfection, 2×10^6 cells were plated in a T25 cell culture flask. C6/36 cells were transfected with pAc-sgRNA1/2-Cas9 using 25 μl Lipofectamine 2000 (Life Technologies, Grand Island, NY, USA) at 5.0 μg plasmid per 2×10^6 cells. After 3 d, C6/36 cells were collected and genomic DNA was extracted using MiniBEST Universal Genomic DNA Extraction Kit (Takara-Bio, Shiga, Japan), according to the manufacturer's protocol. The edited region was amplified using Q5 Hot Start High-Fidelity 2 × Master Mix (New England Biolabs, Ipswich, MA), 200 ng genomic DNA and the primers NixF and NixR flanking the cut site (Supplementary Table S1). The PCR products were used to detect indel mutations with mismatch-sensitive T7 endonuclease I (T7E1) (New England Biolabs, Ipswich, MA) according to the manufacturer's protocol, and then cloned into pJET1.2/blunt Cloning Vector. These indel mutations were confirmed with sequencing (Sanger et al., 1977), and analyzed with MEGA 7.0 (Kumar et al., 2016).

For knock-in in C6/36 cells, two 80 nt single-stranded oligodeoxynucleotides (ssODN), ssODN1 and ssODN2 were designed (Supplementary Table S2), and the location was shown in Fig. 3C (Yoshimi et al., 2016). The pIE-DsRed-T2A-Puro-SV40 cassette was amplified with Q5 Hot Start High-Fidelity 2 × Master Mix (New

England Biolabs, Ipswich, MA) and primer pair pIEF/SV40R (Supplementary Table S1). PCR products were purified with the GeneJET PCR Purification Kit (Thermo Fisher Scientific, Carlsbad CA, USA) and used as a donor template. C6/36 cells were transfected with the plasmid pAc-sgRNA-Cas9 and the donor template by using Lipofectamine 2000 (Life Technologies, Grand Island, NY, USA) at 2.5 μg plasmid, 2.5 μg donor and each ssODN 3 μl (10 μM) per 2 × 10^6 cells. After 72 h, the cells expressing Cas9 protein were selected using 5 μg/ml puromycin (Life Technologies, Grand Island, NY, USA). Cells expressing red fluorescence were then enriched using Beckman Coulter MoFlo XDP Cell Sorter (Beckman Coulter Inc, Brea, USA) into 200 μl medium in 96-well plates.

2.6. Embryonic micro-injection and phenotypes of knockout mutants

Recombinant Cas9 protein was obtained commercially (CP01, PNA Bio, Newbury Park, CA, USA). Microinjection into embryos was conducted according to the standard protocols (Lobo et al., 2006) with slight modification. Three to four days post blood-feeding, approximately 20 females were transferred into a 400 ml plastic container with a wet filter paper and a pre-soaked cotton under the bottom, and embryos used for micro-injection were collected by placing the container in the dark for 30 min 20–35 embryos were lined up on a Western blot filter paper immersed with microinjection buffer. Microinjection was performed using an InjectMan NI2 (Eppendorf Hauppauge, NY, USA) with a FemtoJet (Eppendorf, Hamburg, Germany) as a pump source, and an ECLIPSE TS100 inverted microscope (Nikon, Tokyo, Japan). A GD-1 glass capillary (NARISHIGE, Tokyo, Japan) with filament were pulled with the PN-30 puller (NARISHIGE, Tokyo, Japan) and grinded with micro grinder EG-400 (NARISHIGE, Tokyo, Japan). All injection mixes were prepared with Cas9 protein (333 ng/μl), purified sgRNA (each at 100 ng/μl), and 1 × injection buffer (Jasinskiene et al., 2007). Injection mixes were injected into embryos, and embryos were allowed to recover and develop for 3–5 days at the standard mosquito-rearing insectary conditions. For the negative control experiment, Cas9 protein alone was injected into embryos. When adults eclosed, phenotypes of knockout mutants were photographed under the SMZ1000 stereomicroscope (Nikon, Tokyo, Japan).

2.7. Analysis of CRISPR-Cas9-induced mutations by high resolution melting assay (HRMA) and sequencing

Genomic DNA was extracted from feminized, malformed and wild-type (WT) mosquitoes using the Universal Genomic DNA Extraction kit (Takara). Primers were designed flanking the putative CRISPR-Cas9 cut site (Supplementary Table S1). Insertion and deletion (Indel) mutants were detected with HRMA, and gDNA from WT male was used as the control. PCR products from the feminized, malformed and several WT mosquitoes were cloned into pGEM-T Easy Vector (Promega Corporation, Madison WI, USA) and sequenced.

2.8. Statistics

All data is presented with mean ± SEM from three independent experiments. Significant differences among the data groups were analyzed in GraphPad Prism 6 using an unpaired *t*-test. P value thresholds were set at 0.01 ($p < 0.01$) for highly significant differences (**).

3. Results

3.1. The Aedes albopictus Nix (AalNix) gene is male-specific and has a complex structure

A partial coding sequence of the *Nix* homolog was reported in the *Ae. albopictus* mosquito (Accession KP765684) and only one exon was described in this partial sequence (Hall et al., 2015a). A presumably

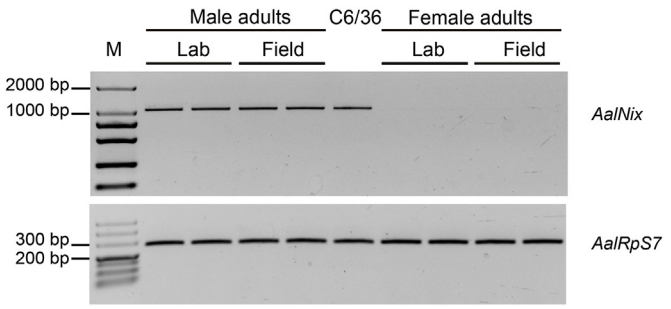

Fig. 1. *Ae. albopictus Nix* (*AalNix*) is male-specific. PCR of *AalNix* using genomic DNA isolated from C6/36 cells, and from male and female *Ae. albopictus* adults of the Foshan (lab) strain and field-collected samples. Amplification of *Ae. albopictus Rps7* (*AalRpS7*) was used as a positive control. Primers NixF and NixR are shown in Supplementary Table S1.

full-length *Nix* gene (LOC109397226) with two exons separated by a short 107 bp intron was later found in the genome assembly of the C6/36 cells, which are apparently derived from a male *Ae. albopictus* source (Miller et al., 2018). LOC109397226 was predicted to encode a 282 aa protein which extends the KP765684 sequence and shows approximately 50% amino acid identity to the *Ae. aegypti* NIX protein (Miller et al., 2018). To confirm the male-specificity of *AalNix*, primers NixF/NixR (Supplementary Table S1) that span the two predicted exons were designed to PCR-amplify genomic DNA isolated from the laboratory Foshan strain and field-collected *Ae. albopictus* adults. *AalNix* can be amplified from male mosquitoes, but not from female mosquitoes (Fig. 1). The results indicate that *AalNix* is male-specific in both laboratory and field-collected *Ae. albopictus*. The same primers also amplified *AalNix* from the genomic DNA of C6/36 cells (Fig. 1), which is consistent with male *Ae. albopictus* as the source of this cell line.

To determine the full-length transcripts of the *AalNix* gene, 5′ and 3′ RACE were performed using RNA from 24 to 48 h postoviposition embryos, male pupae, male adults, and C6/36 cells (Supplementary Table S1). A total of 6 transcripts identified by 5′ and 3′ RACE across these different samples revealed an unexpected complexity of the *AalNix* gene and its splicing (GenBank *AalNix1*: MN364861, *AalNix2*: MN364862, *AalNix3*: MN364863, *AalNix4*: MN364864, *AalNix5*: MN364865, *AalNix6*: MN364866) (Fig. 2A). First, in addition to the previously identified exons 1 and 2, which are homologous to the *Ae. aegypti Nix* despite a much shorter intron size (Hall et al., 2015a; Miller et al., 2018), two additional exons were found in some transcripts (Fig. 2A). When aligning the transcripts with the C6/36 genome sequence, we found that the four exons were separated by 107 bp, 79.8 kb and 89 kb introns, respectively. Second, complex alternative splicing that includes exon skipping and intron retention were observed. In embryos, there are three *AalNix* isoforms (hereafter called *AalNix1-3*), where *AalNix1* includes all 4 exons, *AalNix2* skips exon 2, and *AalNix3* retains intron 1 and terminates within the previously characterized exon 2. These three transcripts encode predicted proteins of 329 aa, 307 aa, and 233 aa, respectively. Only *AalNix1* encodes a protein containing both of the RRM motifs found in the *Ae. aegypti* NIX protein. Out of the above three isoforms, only *AalNix2* and *AalNix3* was found in male pupae, male adults and C6/36 cells. In addition, a fourth isoform *AalNix4* that retains intron 1 but terminates at a slightly different location than *AalNix3* was found in male pupae, male adults and C6/36 cells (Fig. 2A). Finally, two weakly transcribed isoforms, *AalNix5* and *AalNix6* were found to contain the previously described exons 1 and 2 plus a third exon that is located on different scaffolds, (MNAF02001824.1 and MNAF02001902.1) and (MNAF02002029.1 and MNAF02002277.1), respectively. The distance between exon 2 and exon 3 in *AalNix5* and *AalNix6* has not been determined. All six isoforms of *Nix* share exon 1. Motif search based on NCBI's Conserved Domain Database (Marchler-Bauer et al., 2011), showed that all

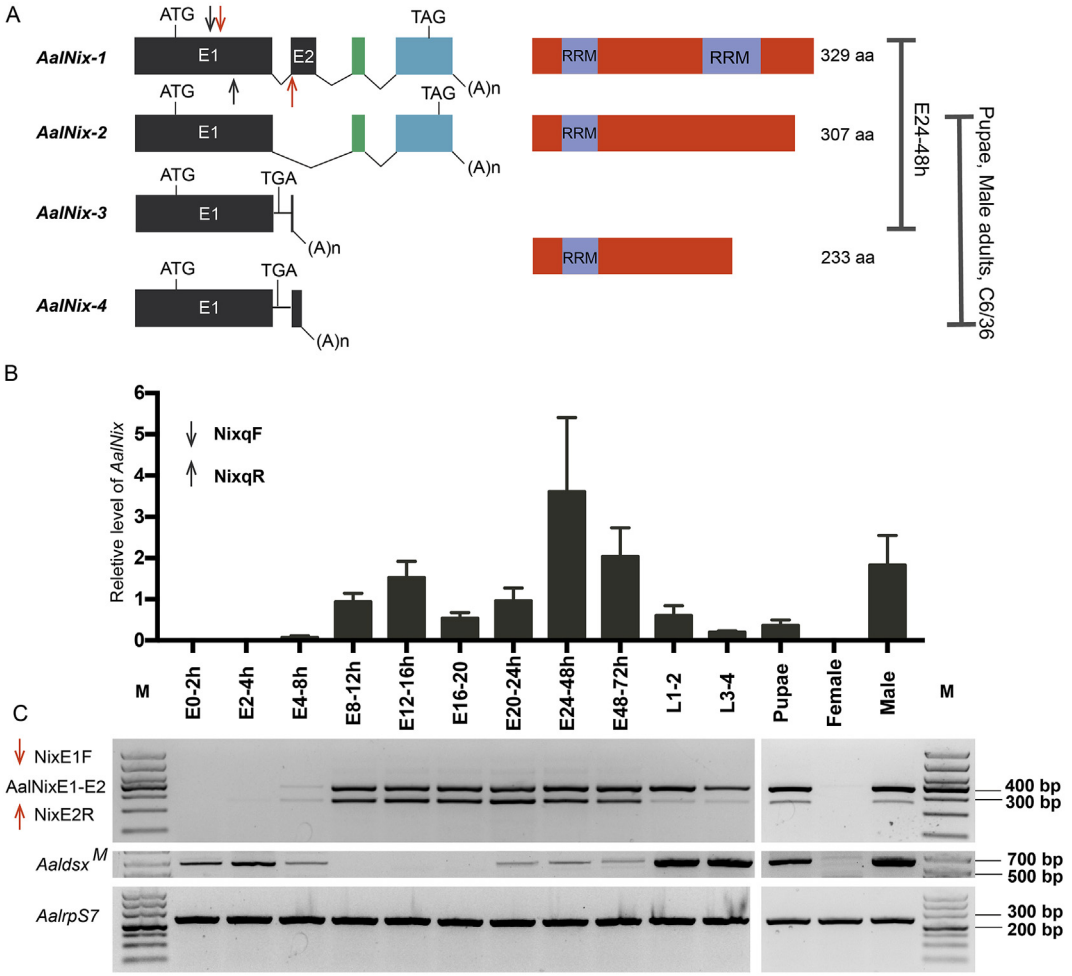

Fig. 2. Isoforms and transcription profile of *AalNix* in *Ae. albopictus*. (A) *AalNix* isoforms identified in embryos between 24 and 48 h after oviposition (*AalNix1-3*), pupae (mixed-sex) (*AalNix2-4*), male adults (*AalNix2-4*) and C6/36 cells (*AalNix2-4*); (A)n indicates Poly(A). The known *AalNix* exons are shown as black boxes, and newly discovered exons are shown as blue and green boxes. Only *AalNix1* has two RRMs, and all the others contain one. Red and black arrows indicate primers used in (C) and (B), respectively. (B) Developmental profile of *AalNix* based on quantitative RT-PCR with primers anchored in exon 1 which have a common amplicon for all isoforms (blacks arrows shown for *AalNix1* in Fig. 2A indicate primers used). Transcription of *AalNix* initiates as early as 4 h after oviposition, and throughout all males' life. The results were normalized to *Ae. albopictus Rps7* (*AalRpS7*) and shown as the mean ± SEM (C) Developmental profile of *AalNix* (upper panel) and *Aaldsx*^{M} (top band in lower panel) based on RT-PCR with intron-spanning primers. As with RT-qPCR results (Fig. 2B), *AalNix* is detected in embryos as early as 4 h after oviposition. The intron between exon 1 and exon 2 shows some retention in early embryos, while after the embryonic stage the intron retention is predominant. Maternally deposited *Aaldsx*^{M} disappears by approximately 8 h, and the zygotic *Aaldsx*^{M} reappears at 20–24 h, after *AalNix* expression. The *AalRpS7* (middle panel) was used as a positive control. The red arrows at left of top panel in (C) indicate primers shown in Fig. 2A used in RT-PCR. NixE2R can bind sequence in *AalNix3-6* corresponding to sequence of Exon 2 shown for *AalNix1* in (A).

isoforms contained one or two RNA binding motifs (RRM) (Fig. 2A and Supplementary Fig. S1).

3.2. *AalNix is expressed in the embryonic and other developmental stages*

To investigate the developmental expression profile of *AalNix*, primer pair NixqF/NixqR located in exon 1 which have a common amplicon for all isoforms for *AalNix1-6* was designed for RT-qPCR (Fig. 2B and Supplementary Table S1) and intron-spanning primers NixE1F/NixE2R for *AalNix1* and *AalNix3-6* were designed for RT-PCR (Fig. 2C and Supplementary Table S1). For the NixqF/NixqR primer pair, the RT-qPCR results showed that *AalNix* initiates expression in embryos between 4 h and 8 h after oviposition, and throughout different life stages (Fig. 2B), which is similar to the expression profile of *Ae. aegypti Nix* (Hall et al., 2015a). In adults where we separated the two sexes, transcription of *AalNix* is limited to male mosquitoes (Fig. 2B). As with RT-qPCR results (Fig. 2B), *AalNix* is detected in embryos as early as 4 h after oviposition by RT-PCR with NixE1F/NixE2R. In early embryos, some intron retention is evident between exon 1 and exon 2 (*AalNix3* and *AalNix4*), while after the embryonic stage intron retention is predominant (Fig. 2C). When the intron is retained, the translation of *Nix* will terminate at stop codon in the intron (Fig. 2A and Supplementary Fig. S1). The intron-spliced product indicates that *AalNix1* and *AalNix5-6* is less abundant after the embryonic stage (Fig. 2A and C and Supplementary Fig. S1). We surveyed the transcription profile of *Aaldsx*^{M} to determine whether *AalNix* expression occurs prior to *Aaldsx*^{M} splicing. As shown in Fig. 2C (top band) and similar to what was shown in *Ae. aegypti* (Salvemini et al., 2011), there is a presumably maternally deposited *Aaldsx*^{M} which disappears by 4–8 h. *Aaldsx*^{M} reappears at 20–24 h, after *AalNix* expression (Fig. 2C). Thus, the timing of *AalNix* expression is consistent with the hypothesis that it may regulate the splicing of the zygotic *Aaldsx*^{M}.

3.3. *Knockout of AalNix, by knocking in a reporter cassette, promotes the alternative splicing of the female isoforms of dsx (dsx*^{F}*) and fru (fru*^{F}*) in C6/36 cells*

To investigate whether *AalNix* regulates the sex determination

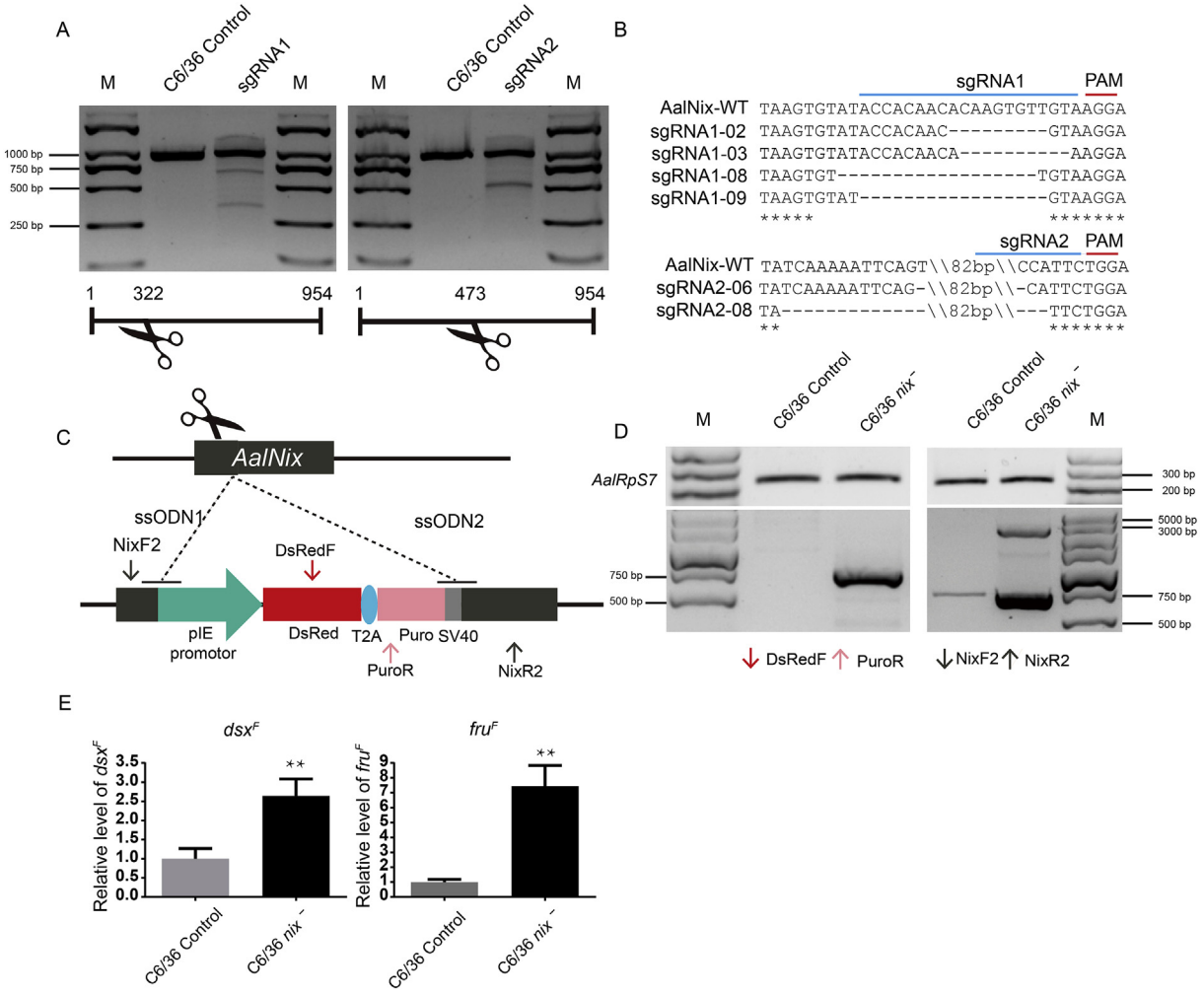

Fig. 3. Knockout of *AalNix* in C6/36 leads to increased dsx^F and fru^F. (A) Surveyor assay detected mutations at the dsDNA break induced by sgRNA1 and sgRNA2. C6/36 control: untreated C6/36 cells; sgRNA1: C6/36 cells transfected with pAc-sgRNA1-Cas9; sgRNA2: C6/36 cells transfected with pAc-sgRNA2-Cas9. (B) Indel mutations confirmed by DNA sequencing. (C) Schematic of knock-in with pIE-DsRed-T2A-Puro and ssODNs. (D) PCR for genomic DNA from control and *nix* knock-out C6/36 cells. The locations of primers are shown in C. (E) Female isoforms of *dsx* and *fru* expression detected with qPCR for control and *nix* knock-out C6/36 cells. The results were normalized to *Ae. albopictus Rps7* (*AalRpS7*) and values are displayed as the mean ± SD of three technical replicates. Two asterisks indicate the 0.001 significance level.

pathway, we studied the impact of *AalNix* knockout on *dsx* and *fru* splicing. First, we used CRISPR/Cas9 to knockout *AalNix* in C6/36 cells, which are clonal male cells (Miller et al., 2018). Two sgRNAs (sgRNA1 and sgRNA2) were designed that target exon 1 of *AalNix* (Supplementary Table S2). After transfection, indel mutations were observed at the cut site based on the surveyor assay, suggesting that these two sgRNAs worked well in C6/36 cells (Fig. 3A and B). However, it is difficult to enrich for mutated cells. Thus, we designed a knock-in selection cassette containing a Puromycin resistance gene and a fluorescent marker DsRed (Fig. 3C) (Yoshimi et al., 2016). After transfection and selection with antibiotics, we found that the cassette had integrated at the sgRNA1 cut site (Fig. 3C). In cells that are selected with puromycin and sorted by Fluorescence Activated Cell Sorting (FACS) according to dsRED (Fig. 3D), we observed that female isoforms of *dsx* and *fru* increased 2.63 ± 0.45 and 7.44 ± 1.39 fold compared to unmodified C6/36 control cells, respectively (Fig. 3E). These results indicate that *AalNix* is involved in the sex determination pathway as an upstream regulator of *dsx* and *fru* splicing.

3.4. Somatic knockout of AalNix results in feminization of males and alters dsx and fru splicing in Aedes albopictus

To further investigate the function of *AalNix*, single sgRNA and dual sgRNA guided CRISPR/Cas9 were conducted to knock out the shared exon 1 of *AalNix* in *Ae. albopictus*. In the single sgRNA guided CRISPR/Cas9 experiments, *in vitro* synthesized sgRNA1 or sgRNA2 was injected with Cas9 protein into *Ae. albopictus* embryos, respectively. G_0 mutants showing feminization or deformities in sexually dimorphic organs were observed (Fig. 4). All these individuals contain the *AalNix* gene, thus confirming that they are genetically male (Fig. 5). We define deformities as genitals rotated from the normal orientation, and feminization as feminized antennae, absence or partial absence of gonocoxites, gonostyli, testes and accessory glands, and the formation of ovaries. The phenotype of feminization or deformities for each male was recorded (Table 1). For the embryos injected with sgRNA1 and the Cas9 protein, 213 pupae eclosed as adults, and 30 of these individuals showed either feminization or deformities (Table 1). Twenty five of the 30 (83%) had normal antennae but their genital rotated 90° (Fig. 4C and Table 1). Five of the 30 (16.7%) showed feminized antenna with fewer and shorter setae than normal males and their gonocoxite and gonostyli were partly absent (Fig. 4D and Table 1). For the embryos injected with

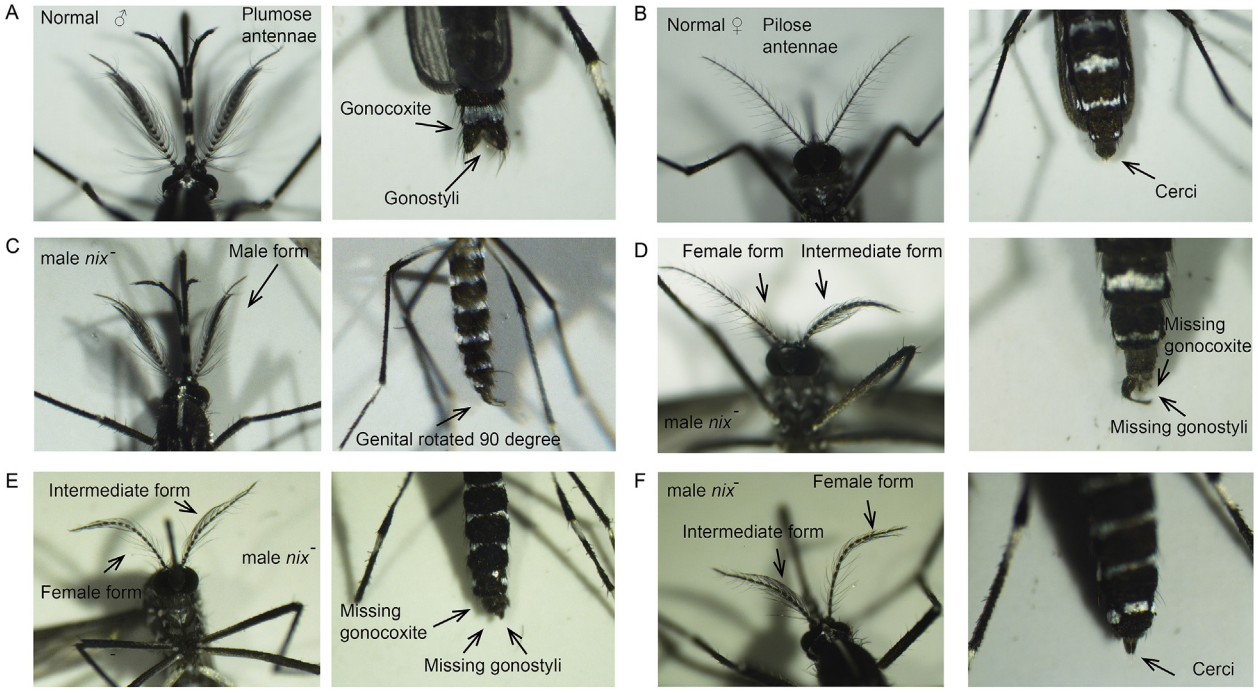

Fig. 4. Representative images showing feminization and external deformities in sexually dimorphic organs that result from CRISPR/Cas9-induced disruption of *AalNix*. These images are from the experiments of single sgRNA-guided knockout. (A) WT male: plumose antennae, genitals with gonocoxites and gonostyli. (B) WT female: pilose antennae, genitals with cerci. (C) nix^{-} male: plumose antennae, genital rotated 90°. (D) *nix*$^{-}$ male: both sides have fewer setae than normal males; one side is pilose antennae and the other side is intermediate. One side of the genitalia is missing gonocoxites and gonostyli. (E) *nix*$^{-}$ male: both sides have fewer setae than normal males; one side is pilose antennae and the other side is intermediate. One side lacks gonocoxites and both sides lack gonostyli. (F) *nix*$^{-}$ male: both sides have fewer setae than normal males; one side is pilose antennae and other side is intermediate, genitals have cerci.

sgRNA2 and the Cas9 protein, 279 pupae eclosed into adults, and 67 individuals showed feminization or deformities (Table 1). Fifty seven of the 67 (85%) had normal male antennae but their genitals rotated 90° (Fig. 4C and Table 1). Ten of the 67 (15%) had feminized antenna with fewer and shorter setae than normal males and their gonocoxite and gonostyli were partly absent (Fig. 4D and Table 1). Non-homologous end joining (NHEJ) will introduce insertion or deletion (Indel) mutations at the Cas9 cleavage site. Indel mutations can be detected by High Resolution Melting Analysis (HRMA) due to a change in the melting profile of the PCR product encompassing the Indel, compared to the nonmutated control. Mutations were detected at the Cas9 cleavage sites by HRMA using individuals that showed feminization or deformities in sexually dimorphic organs (Fig. 5A and B). We detected mutations in 2 and 8 individuals in the sgRNA1 and sgRNA2 groups, respectively, having feminization or deformity phenotypes. These mutations were confirmed by DNA sequencing, and some of these mutations are shown in Fig. 5A and C, and Supplementary Fig. S2. The female isoforms of *dsx* and *fru* increased while the male isoforms of *dsx* and *fru* decreased in the *AalNix* knockout male individual, compared to wild-type individuals (Fig. 5E). Although fru^{F} expression was only slightly increased in the *Nix* knockout individuals, it was statistically different from the control group ($p = 0.03$).

For the embryos co-injected with both sgRNA1, sgRNA2 and the Cas9 protein, 246 pupae eclosed into adults, and 36 individuals showed feminization or deformities (Table 1 and Supplementary Table S3). Nine out of the 36 (25%) had normal antennae and their genitals rotated 90° (Fig. 4C, Table 1 and Supplementary Table S3). One of the 36 had normal antennae and its genitals appeared malformed (Table 1 and Supplementary Table S3). Eight of the 36 (22%) had normal antennae but their gonocoxite and gonostyli are either absent or partly absent (Table 1 and Supplementary Table S3). Fourteen of the 36 (39%) showed that either one side or both side of the antennae have fewer setae than normal and their gonocoxite and gonostyli were either absent or partly absent (Fig. 4D and E, Table 1 and Supplementary Table S3). Two of the 36 (5.6%) showed that either one side or both side of the antennae have fewer setae than normal and their genitals were rotated 180° (Table 1 and Supplementary Table S3). Two of the 36 (5.6%) had feminized antenna with fewer and shorter setae than normal males and their genitals appeared feminized (Fig. 4F, Table 1 and Supplementary Table S3). When dissecting these individuals, we found that sixteen of the 36 (44.4%) showed feminization such as partial or total absence of testes and accessory glands, or presence of ovaries (Fig. 6 and Supplementary Table S3). For the control group when only the Cas9 protein was injected, 103 pupae emerged as adults, and no individuals showed feminization or deformities (Table 1). We chose 20 individuals with atypical sex phenotype for HRMA, namely *nix*$^{-}$ 1, *nix*$^{-}$ 2, *nix*$^{-}$ 3, *nix*$^{-}$ 5, *nix*$^{-}$ 6, *nix*$^{-}$ 7, *nix*$^{-}$ 8, *nix*$^{-}$ 11, *nix*$^{-}$ 14, *nix*$^{-}$ 17, *nix*$^{-}$ 18, *nix*$^{-}$ 20, *nix*$^{-}$ 22, *nix*$^{-}$ 23, *nix*$^{-}$ 24, *nix*$^{-}$ 25, *nix*$^{-}$ 28, *nix*$^{-}$ 29, *nix*$^{-}$ 35, and *nix*$^{-}$ 36 (Fig. 7A and Supplementary Table S3). All these individuals contain the *AalNix* gene, thus confirming that they are genetically male (Fig. 7A and Supplementary Table S3). Among them, only *nix*$^{-}$ 25 showed mutations at the sgRNA1 site, while 15 individuals showed sgRNA2-mediated mutations including *nix*$^{-}$ 2, *nix*$^{-}$ 3, *nix*$^{-}$ 6, *nix*$^{-}$ 7, *nix*$^{-}$ 8, *nix*$^{-}$ 11, *nix*$^{-}$ 14, *nix*$^{-}$ 17, *nix*$^{-}$ 18, *nix*$^{-}$ 20, *nix*$^{-}$ 22, *nix*$^{-}$ 25, *nix*$^{-}$ 28, *nix*$^{-}$ 29, and *nix*$^{-}$ 35 (Fig. 7A and Supplementary Table S3). Eleven mosquitoes were selected for sequencing, and all these individuals showed mutations at the Cas9 cleavage site, among which *nix*$^{-}$ 3, *nix*$^{-}$ 18, *nix*$^{-}$ 25 and *nix*$^{-}$ 28 had relatively high mutation rates (Fig. 7B and Supplementary Fig. S2). Although there are large variations in relative expression levels of *dsx* and *fru* isoforms among samples including some wild-type controls, the ratio of dsx^{F}/dsx^{M} (Fig. 7C) and fru^{F}/fru^{M} (Fig. 7D) increased in *nix*$^{-}$ individuals (Supplementary Table S4). Among the individuals with a high mutation rate (*nix*$^{-}$ 3, *nix*$^{-}$ 18, *nix*$^{-}$ 25 and *nix*$^{-}$ 28), the transformation of *dsx* and *fru* to the female isoform was more pronounced. Large variations among individuals may reflect variations in the degree of somatic mutations in the *nix*$^{-}$ individuals. Thus, all three independent experiments (Figs. 3, 5 and 7) suggest that *AalNix* is a male-determining factor that functions as an upstream regulator of *dsx*

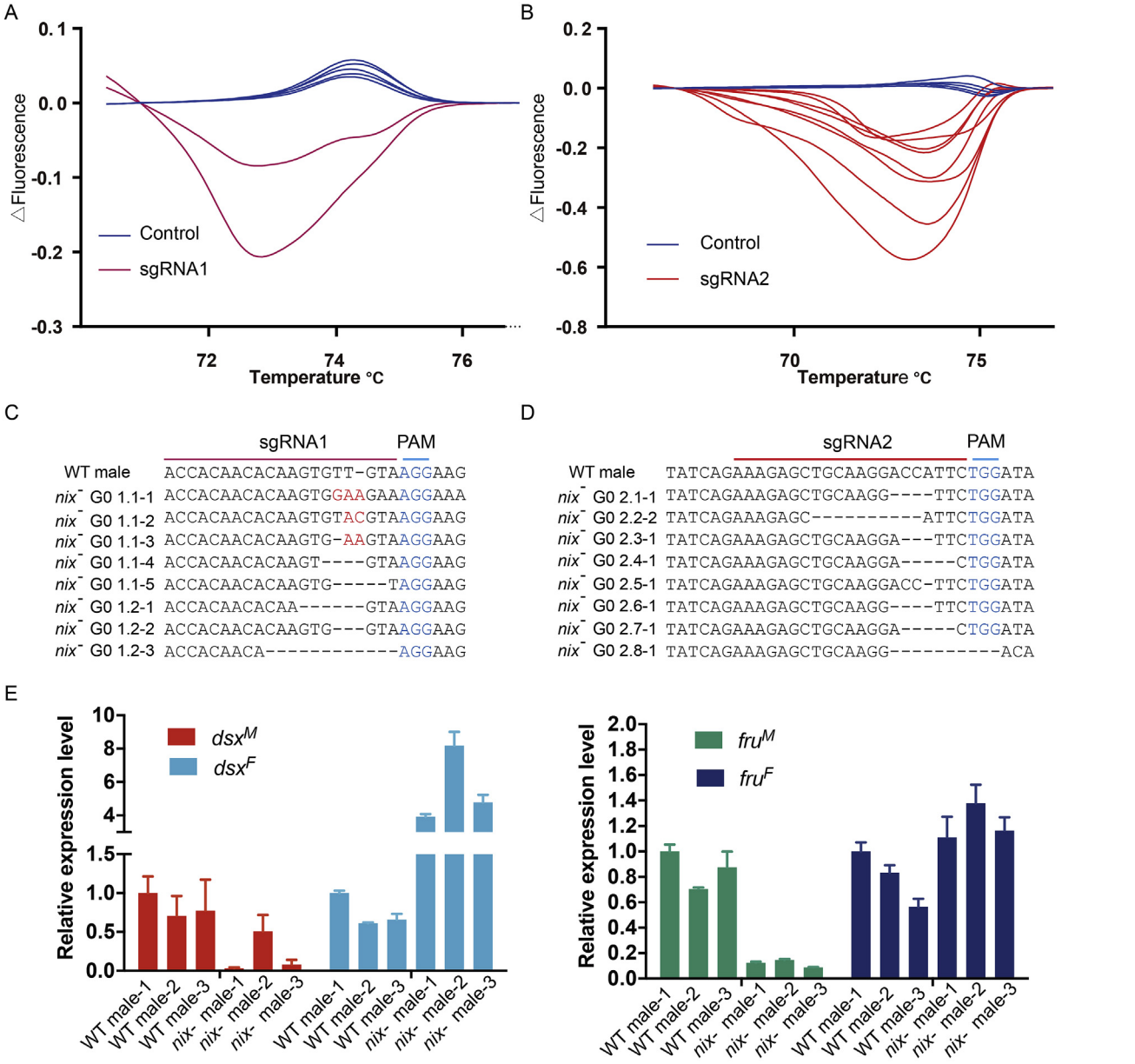

Fig. 5. Single sgRNA CRISPR/Cas9 induces mutations in *AalNix* and changes the sex-specific splicing of *dsx* and *fru*. Mutations were confirmed with high resolution melt analysis (HRMA) and DNA sequencing. (A) sgRNA1: Change in fluorescence of feminized males (red lines) relative to control WT males (blue lines). (B) sgRNA2, same as in A. (C) Sequencing of sgRNA1-induced mutations in the *AalNix* gene. PCR products spanning the sgRNA target sites were analyzed for indel mutations. The first line in each alignment represents the wild-type sequence, and subsequent lines show individual mutant clones. Deleted bases are marked with dashes and inserted or substituted bases are indicated in red. Nix- G0 x.y–z: x refers to the sgRNA; y is the individual number; z is the clone number. (D) Sequencing of sgRNA2-induced mutations in the *nix* gene, all symbols are as in c. (E) The relative expression of dsx^F, dsx^M (left panel), $fru^F$and fru^M (right panel) in three wild-type males and three nix$^-$ male individuals. The results were normalized to *Ae. albopictus Rps7* (*AalRpS7*). All the individuals were compared with WT male-1 and values are shown as the mean ± SD of three technical replicates.

and *fru* splicing in *Ae. albopictus*.

4. Discussion

Aedes albopictus is an aggressive biting species that has spread worldwide from its native range in Asia in the last 30–40 years (Kotsakiozi et al., 2017). Together with *Ae. aegypti*, they represent two of the most important vectors for arboviruses that cause dengue, chikungunya, and Zika fever. There has been longstanding interest to understand the molecular mechanism of sex determination in mosquitoes for both basic biology and potential applications. For example, genetic manipulations of the sex determination pathway could potentially reduce the number of biting females and reduce a target population (Adelman and Tu, 2016; Criscione et al., 2016; Kyrou et al., 2018). A male-determining factor *Nix* has been previously shown to specify male development in *Ae. aegypti*. In this study we have shown that *Nix* also functions as a male-determining factor in *Ae. albopictus*. Therefore, the potential for controlling arboviral diseases by manipulating the *Nix*-regulated sex determination pathway has been expanded to an important vector species.

The evidence that supports *AalNix* as a male-determining factor includes its male-specificity, its expression profile, and the impact of the loss of function mutations. Loss of function mutations were achieved by CRISPR/Cas9-mediated knockouts of *AalNix* both by embryonic injections and by transfection of a male *Ae. albopictus* cell line C6/36. During independent sets of experiments with different sgRNAs targeting the

Table 1
Efficiency and phenotype of *Nix* knockout in *Ae. albopictus* males.

Group	Embryo	Larvae	Pupae	Female adult (% of all adults)	Male adult (% of all adults)	Feminized or deformed males
sgRNA1 + Cas9	609	289	228	104 (48.83%)	109 (51.17%)	30 (25[a], 5[b])
sgRNA2 + Cas9	805	371	310	157 (56.27%)	122 (43.73%)	67 (57[a], 10[c])
sgRNA1 + sgRNA2 + Cas9	996	286	263	129 (52.44%)	117 (47.56%)	36 (9[a], 1[d], 8[e], 14[f], 2[g], 2[h])
Cas9 protein alone	490	114	103	54 (52.43%)	49 (47.57%)	0

[a] Normal antennae, genitals rotated 90°.
[b] Both antennae have fewer setae than normal, gonocoxite and gonostyli partly absent.
[c] Both antennae have fewer setae than normal, gonocoxite and gonostyli absent or partly absent.
[d] Normal antennae, genitals appear malformed.
[e] Normal antennae, gonocoxite and gonostyli absent or partly absent.
[f] One side or both side antennae have fewer setae than normal, gonocoxite and gonostyli absent or partly absent.
[g] One side or both side antennae have fewer setae than normal, genitals rotated 180°.
[h] Both antennae have fewer setae than normal, genitals appear malformed.

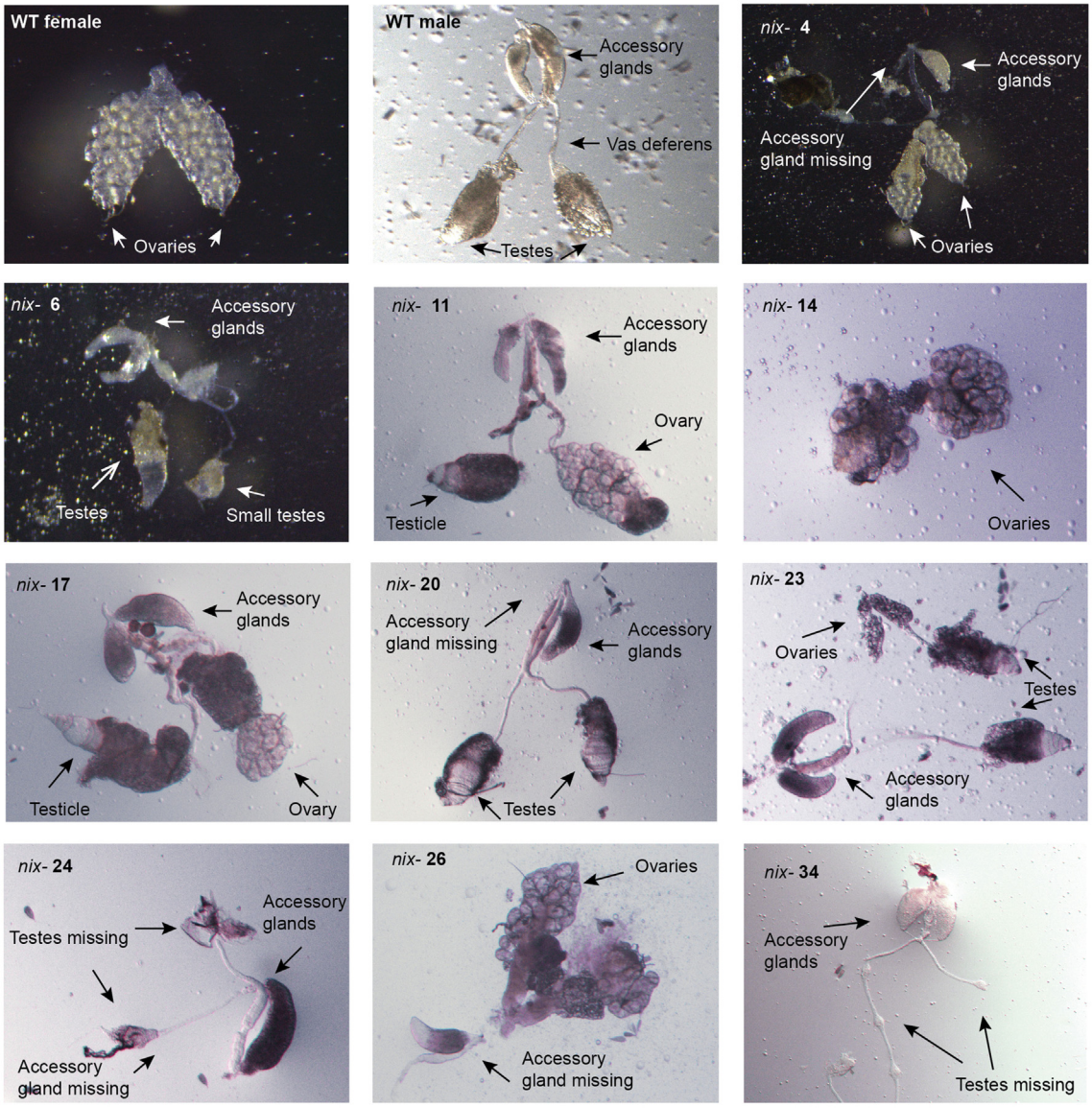

Fig. 6. CRISPR-Cas9-induced disruption of *AalNix* causes deformities and feminization in internal reproductive organs in male mosquitoes. All individuals with feminized and malformed external phenotypes were dissected to observe the internal phenotype. WT female and WT male are from individuals that were injected with only the Cas9 protein. *nix*$^{-}$ G_0 individuals are from the dual sgRNA-guided knockout experiment. *nix*$^{-}$ x: x is the numbering used to indicate the individual mosquito.

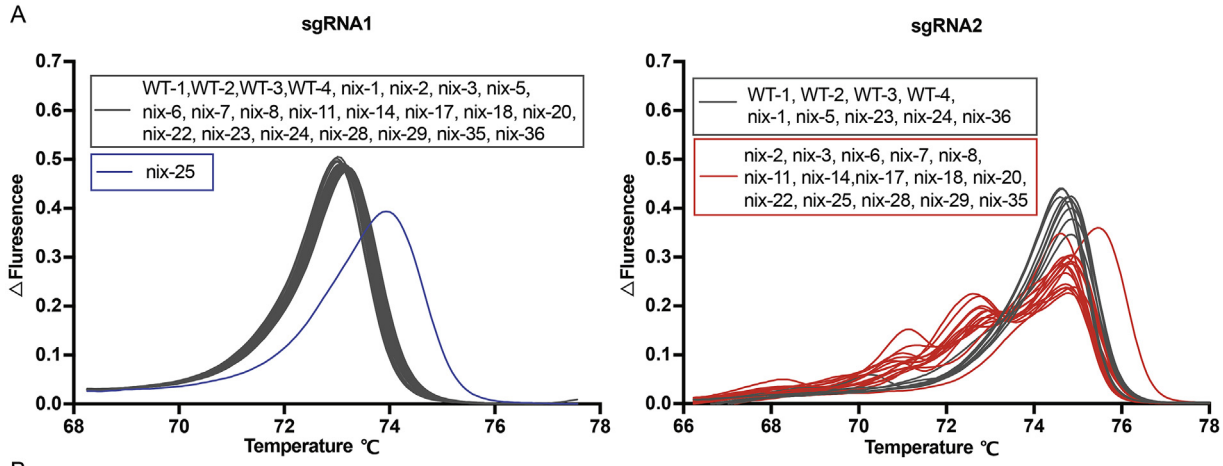

B

	PAM sgRNA1 CCTTACAACACTTGTGTTGTGGT	sgRNA2 PAM AAGAGCTGCAAGGACCATTCTGG
nix WT	TTTTGTGATGTGAAA//121//TTCTTCCTTACAACACTTGTGTTGTGGTATACA//107bp//TCAGAAAGAGCTGCAAGGACCATTCTGGATA	
nix- 3 upper band	TTTTGTGATGTGAAA//121//TTCTTCCTTACAACACTTGTGTTGTGGTATACA//107bp//TCAGAAAGAGCTGCAAGGACCATTCTGGATA	5/12
nix- 3 upper band	TTTTGTGATGTGAAA//121//TTCTTCCTTACA----------CA//107bp//TCAGAAAGAGCTGCAAGGACCATTCTGGATA	6/12
nix- 3 upper band	TTTTGTGATGTGAAA//121//TTCTTCCTTACA----------CA//107bp//TCAGAAAGAGCTG---------TTCTGGATA	1/12
nix- 3 lower band	TTTTGTGATG----------GATA	11/11

	PAM sgRNA1 CCTTACAACACTTGTGTTGTGGT	sgRNA2 PAM AAGAGCTGCAAGGACCA-------TTCTGG
nix WT	AATTACTTTCTTCCTTACAACACTTGTGTTGTG//115bp//CAGAAAGAGCTGCAAGGACCA-------TTCTGGATACTAAGCCTACA	
nix- 18 upper band	AATTACTTTCTTCCTTACAACACTTGTGTTGTG//115bp//CAGAAAGAGCTGCAAGGTCACTAAGCCTACAAGGATACTAAGCCTACA	9/15
nix- 18 upper band	AATTACTTTCTTCCTTACAACACTTGTGTTGTG//115bp//CAGAAAGAGCTGCAAGGACC--------TTCTGGATACTAAGCCTACA	4/15
nix- 18 upper band	AATTACTTTCTTCCTTACAACACTTGTGTTGTG//115bp//CAGAAAGAGCTGCAAGGAC---------TTCTGGATACTAAGCCTACA	1/15
nix- 18 upper band	AATTACTTTCTTCCTTACAACACTTGTGTTGTG//115bp//CAGAAAGAGCT----------TTCTGGATACTAAGCCTACA	1/15
nix- 18 upper band	AATTACTTTCTTCCTTA----------TTGTG//115bp//CAGAAAGAGCTGCAAGGACCA------ATTCTGGATACTAAGCCTACA	1/6
nix- 18 middle band	AATTACTTTCTTCCTTA----------TTGTG//115bp//CAGAAAGAGCTGCAAGGACCA-------TTCTGGATACTAAGCCTACA	4/6
nix- 18 middle band	AATTACTTTCTTCCTTA----------TTGTG//115bp//CAGAAAGAGCTGCAA----------GGAC-CTAAGCCTACA	1/6
nix- 18 lower band	AATTACTTTCTTCCTTA----------CTGGATACTAAGCCTACA	4/19
nix- 18 lower band	AATTACTTTCTTCCT----------GGATACTAAGCCTACA	15/19

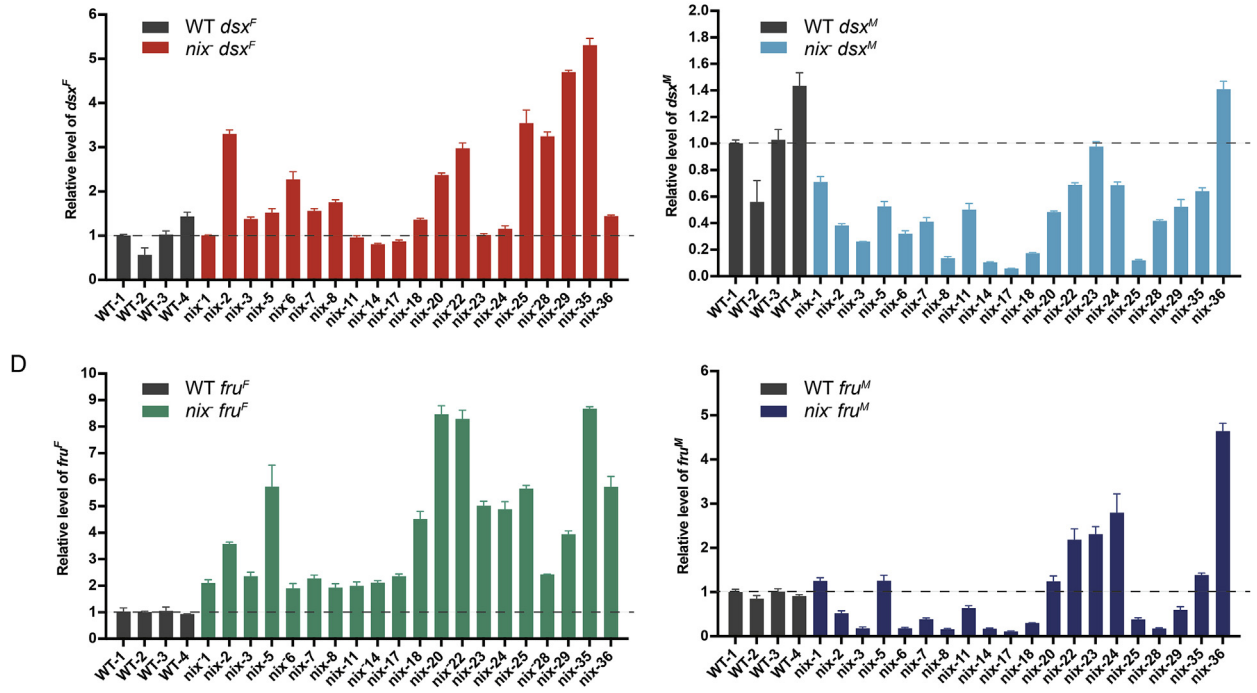

(caption on next page)

Fig. 7. Dual sgRNA CRISPR/Cas9 induces mutations in *AalNix* and changes the sex-specific splicing of *dsx* and *fru*. Mutations were confirmed with high resolution melt analysis (HRMA) and DNA sequencing. (A) sgRNA1 and sgRNA2 target site indel detection by HRMA after sgRNA1-sgRNA2-Cas9 protein co-injection. (B) Sequencing mutations in the sgRNA1 and sgRNA2 sites of *AalNix* gene. PCR products spanning the sgRNA target sites were analyzed for indel mutations. The first line in each alignment represents the wild-type sequence, and subsequent lines show individual mutant clones. Deleted bases are marked with dashes and inserted or substituted bases are indicated in blue. Unmutated clones were highlighted in red. The number to the right of the sequences represents the proportion of each mutant type in all sequenced clones. The relative expression of dsx^F, dsx^M (C), $fru^F$and fru^M (D) in wild-type males (only Cas9 protein injection) and nix$^-$ male individuals. The results were normalized to *Ae. albopictus Rps7* (*AalRpS7*). All individuals were compared with WT male-1 and values are shown as the mean ± SD of three technical replicates.

shared exon 1 of *AalNix*, G_0 knockout males consistently showed feminization and deformity including feminized antennae, absence or partial absence of gonocoxites, gonostyli, testes and accessory gland, and the formation of ovaries. It is thus clear that *AalNix* is required for male development. During these *in vivo* knockout experiments, the female isoforms of *dsx* and *fru* increased while the male isoforms of *dsx* and *fru* decreased in the *AalNix* knockout male individuals, compared to wild-type individuals (Figs. 5E and Fig. 7C–D). Moreover, CRISPR/Cas9-mediated knockouts of *AalNix* in the male *Ae. albopictus* cell line C6/36 resulted in increased female isoforms of *dsx* and *fru* compared to wildtype C6/36 cells. Thus, *AalNix* is a male determining factor that functions as an upstream regulator of *dsx* and *fru* splicing in *Ae. albopictus*. In this regard, *AalNix* transcription starts at 4–8 h post-oviposition, which is initiated prior to the establishment of zygotic $AalDsx^M$, which starts to appear at 20–24 h post-oviposition. Taking together all above evidence, we can conclude that despite ~70 MY of divergence, the function of *Nix* as a male determining factor is conserved between *Ae. aegypti* and *Ae. albopictus*. Future experiments in which ectopic expression of *AalNix* is performed in female *Ae. albopictus* will show whether *AalNix* is sufficient to initiate male differentiation.

The *AalNix* isoform that shares the two conserved exons with the *AaeNix* shows approximately 50% identity at the amino acid level with *AaeNix*. *AaeNix* contains one 958 bp isoform with a single 100 kb intron located after 782 bp in the *Nix* cDNA (GenBank KF732822) in the male adults (Hall et al., 2015b; Matthews et al., 2018). Although a further improved *A. albopictus* genome assembly is needed to fully characterize the *AalNix* gene structure, current evidence suggests that the gene structure of *AalNix* may be more complex than what has been reported for *AaeNix*. We isolated multiple cDNA isoforms from *A. albopictus* and the deduced exons all have matching genomic DNA alignments and the predicted exon-intron boundaries are consistent with the consensus of splice junctions. In addition to the previously identified exons 1 and 2, which are homologous to the *Ae. aegypti Nix* (Hall et al., 2015a; Miller et al., 2018), two additional exons are found (Fig. 2A). The existence of exon skipping causes *AalNix2* to lack exon 2. Due to intron retention, *AalNix3* and *AalNix4* are terminated prematurely during translation, thus producing the same protein. A somewhat intriguing discovery was that two weakly transcribed isoforms, *AalNix5* and *AalNix6* were found to contain the previously described exons 1 and 2 plus a third exon that is located on different scaffolds, respectively. The biological significance of these complex splicing patterns is not yet clear. All six isoforms of *Nix* share exon 1, which is why we targeted this exon for loss of function analysis. Future experiments that decipher possibly distinct functions of the *AalNix* isoforms will likely reveal new insights into the evolution of *Nix* and the sex determination pathway in mosquitoes.

Author contributions

PL, data curation, formal analysis, validation, investigation, visualization, article drafting and revision. XL, data curation, formal analysis and article drafting. BJ, data curation, formal analysis, validation, investigation, visualization. JG, conception and design, analysis and interpretation of data. JB, analysis and interpretation of data, article revision. YZ, data curation. ZT, conception and design, analysis and interpretation of data, article revision. XC, conception and design, analysis and interpretation of data, article revision.

Declaration of competing interest

The authors declare no competing financial interests.

Acknowledgements

This work is supported by a combination of funding from the: National Natural Science Foundation of China of China (81420108024, 81829004), National Institutes of Health, USA (AI136850, AI123338) and Natural Science Foundation of Guangdong Province (2014A030312016). We thank J.L Liu for pAc-sgRNA-Cas9, which was obtained through addgeneg.org.

Appendix A. Supplementary data

Supplementary data to this article can be found online at https://doi.org/10.1016/j.ibmb.2019.103311.

References

Adelman, Z.N., Tu, Z., 2016. Control of mosquito-borne infectious diseases: sex and gene drive. Trends Parasitol. 32, 219–229.
Bachtrog, D., Mank, J.E., Peichel, C.L., Kirkpatrick, M., Otto, S.P., Ashman, T.L., Hahn, M.W., Kitano, J., Mayrose, I., Ming, R., Perrin, N., Ross, L., Valenzuela, N., Vamosi, J.C., Tree of Sex, C., 2014. Sex determination: why so many ways of doing it? PLoS Biol. 12, e1001899.
Bassett, A.R., Tibbit, C., Ponting, C.P., Liu, J.L., 2014. Mutagenesis and homologous recombination in Drosophila cell lines using CRISPR/Cas9. Biology Open 3, 42–49.
Biedler, J., Tu, Z., 2016. Chapter two-sex determination in mosquitoes. Adv. Insect Physiol. 51, 37–66.
Bopp, D., Saccone, G., Beye, M., 2014. Sex determination in insects: variations on a common theme. Sex. Dev. 8, 20–28 genetics, molecular biology, evolution, endocrinology, embryology, and pathology of sex determination and differentiation.
Criscione, F., Qi, Y., Saunders, R., Hall, B., Tu, Z., 2013. A unique Y gene in the Asian malaria mosquito Anopheles stephensi encodes a small lysine-rich protein and is transcribed at the onset of embryonic development. Insect Mol. Biol. 22, 433–441.
Criscione, F., Qi, Y.M., Tu, Z.J., 2016. GUY1 confers complete female lethality and is a strong candidate for a male-determining factor in Anopheles stephensi. Elife 5.
Gempe, T., Beye, M., 2011. Function and evolution of sex determination mechanisms, genes and pathways in insects. Bioessays 33, 52–60 news and reviews in molecular, cellular and developmental biology.
Gilchrist, B.M., Haldane, J.B.S., 1947. Sex linkage and sex determination in a mosquito, culex-molestus. Hereditas 33, 175–190.
Gomulski, L.M., Mariconti, M., Di Cosimo, A., Scolari, F., Manni, M., Savini, G., Malacrida, A.R., Gasperi, G., 2018. The Nix locus on the male-specific homologue of chromosome 1 in Aedes albopictus is a strong candidate for a male-determining factor. Parasites Vectors 11, 647.
Hall, A.B., Basu, S., Jiang, X., Qi, Y., Timoshevskiy, V.A., Biedler, J.K., Sharakhova, M.V., Elahi, R., Anderson, M.A., Chen, X.-G., 2015a. A male-determining factor in the mosquito Aedes aegypti. Science 348, 1268–1270.
Hall, A.B., Basu, S., Jiang, X., Qi, Y., Timoshevskiy, V.A., Biedler, J.K., Sharakhova, M.V., Elahi, R., Anderson, M.A., Chen, X.G., Sharakhov, I.V., Adelman, Z.N., Tu, Z., 2015b. SEX DETERMINATION. A male-determining factor in the mosquito Aedes aegypti. Science 348, 1268–1270.
Hasselmann, M., Gempe, T., Schiott, M., Nunes-Silva, C.G., Otte, M., Beye, M., 2008. Evidence for the evolutionary nascence of a novel sex determination pathway in honeybees. Nature 454, 519–522.
Jasinskiene, N., Juhn, J., James, A.A., 2007. Microinjection of A. aegypti embryos to obtain transgenic mosquitoes. J. Vis. Exp. : J. Vis. Exp. 219.
Kim, J.H., Lee, S.R., Li, L.H., Park, H.J., Park, J.H., Lee, K.Y., Kim, M.K., Shin, B.A., Choi, S.Y., 2011. High cleavage efficiency of a 2A peptide derived from porcine teschovirus-1 in human cell lines, zebrafish and mice. PLoS One 6, e18556.
Kiuchi, T., Koga, H., Kawamoto, M., Shoji, K., Sakai, H., Arai, Y., Ishihara, G., Kawaoka, S., Sugano, S., Shimada, T., Suzuki, Y., Suzuki, M.G., Katsuma, S., 2014. A single female-specific piRNA is the primary determiner of sex in the silkworm. Nature 509,

633.
Kotsakiozi, P., Richardson, J.B., Pichler, V., Favia, G., Martins, A.J., Urbanelli, S., Armbruster, P.A., Caccone, A., 2017. Population genomics of the Asian tiger mosquito, Aedes albopictus: insights into the recent worldwide invasion. Ecol. Evol. 7, 10143–10157.
Krzywinska, E., Dennison, N.J., Lycett, G.J., Krzywinski, J., 2016. A maleness gene in the malaria mosquito Anopheles gambiae. Science 353, 67–69.
Kumar, S., Stecher, G., Tamura, K., 2016. MEGA7: molecular evolutionary genetics analysis version 7.0 for bigger datasets. Mol. Biol. Evol. 33, 1870–1874.
Kyrou, K., Hammond, A.M., Galizi, R., Kranjc, N., Burt, A., Beaghton, A.K., Nolan, T., Crisanti, A., 2018. A CRISPR-Cas9 gene drive targeting doublesex causes complete population suppression in caged Anopheles gambiae mosquitoes. Nat. Biotechnol. 36, 1062–1066.
Lobo, N.F., Clayton, J.R., Fraser, M.J., Kafatos, F.C., Collins, F.H., 2006. High efficiency germ-line transformation of mosquitoes. Nat. Protoc. 1, 1312–1317.
Marchler-Bauer, A., Lu, S., Anderson, J.B., Chitsaz, F., Derbyshire, M.K., DeWeese-Scott, C., Fong, J.H., Geer, L.Y., Geer, R.C., Gonzales, N.R., Gwadz, M., Hurwitz, D.I., Jackson, J.D., Ke, Z., Lanczycki, C.J., Lu, F., Marchler, G.H., Mullokandov, M., Omelchenko, M.V., Robertson, C.L., Song, J.S., Thanki, N., Yamashita, R.A., Zhang, D., Zhang, N., Zheng, C., Bryant, S.H., 2011. CDD: a Conserved Domain Database for the functional annotation of proteins. Nucleic Acids Res. 39, D225–D229.
Marin, I., Baker, B.S., 1998. The evolutionary dynamics of sex determination. Science 281, 1990–1994.
Matthews, B.J., Dudchenko, O., Kingan, S.B., Koren, S., Antoshechkin, I., Crawford, J.E., Glassford, W.J., Herre, M., Redmond, S.N., Rose, N.H., 2018. Improved reference genome of Aedes aegypti informs arbovirus vector control. Nature 563, 501.
McClelland, G., 1962. Sex-linkage in Aedes aegypti. Trans roy Soc trop Med Hyg 56.
Miller, J.R., Koren, S., Dilley, K.A., Puri, V., Brown, D.M., Harkins, D.M., Thibaud-Nissen, F., Rosen, B., Chen, X.G., Tu, Z., Sharakhov, I.V., Sharakhova, M.V., Sebra, R., Stockwell, T.B., Bergman, N.H., Sutton, G.G., Phillippy, A.M., Piermarini, P.M., Shabman, R.S., 2018. Analysis of the Aedes albopictus C6/36 genome provides insight into cell line utility for viral propagation. GigaScience 7.
Papathanos, P.A., Bossin, H.C., Benedict, M.Q., Catteruccia, F., Malcolm, C.A., Alphey, L., Crisanti, A., 2009. Sex separation strategies: past experience and new approaches. Malar. J. 8 (Suppl. 2), S5.
Park, J., Bae, S., Kim, J.S., 2015. Cas-Designer: a web-based tool for choice of CRISPR-Cas9 target sites. Bioinformatics 31, 4014–4016.
Salvemini, M., Mauro, U., Lombardo, F., Milano, A., Zazzaro, V., Arcà, B., Polito, L.C., Saccone, G., 2011. Genomic organization and splicing evolution of the doublesex gene, a Drosophila regulator of sexual differentiation, in the dengue and yellow fever mosquito Aedes aegypti. BMC Evol. Biol. 11 41-41.
Salz, H.K., Erickson, J.W., 2010. Sex determination in Drosophila: the view from the top. Fly 4, 60–70.
Sanchez, L., 2008. Sex-determining mechanisms in insects. Int. J. Dev. Biol. 52, 837–856.
Sanger, F., Nicklen, S., Coulson, A.R., 1977. DNA sequencing with chain-terminating inhibitors. In: Proceedings of the National Academy of Sciences of the United States of America. 74. pp. 5463–5467.
Schutt, C., Nothiger, R., 2000. Structure, function and evolution of sex-determining systems in Dipteran insects. Development (Camb.) 127, 667–677.
Sharma, A., Heinze, S.D., Wu, Y., Kohlbrenner, T., Morilla, I., Brunner, C., Wimmer, E.A., van de Zande, L., Robinson, M.D., Beukeboom, L.W., Bopp, D., 2017. Male sex in houseflies is determined by Mdmd, a paralog of the generic splice factor gene CWC22. Science 356, 642–645.
Varjak, M., Maringer, K., Watson, M., Sreenu, V.B., Fredericks, A.C., Pondeville, E., Donald, C.L., Sterk, J., Kean, J., Vazeille, M., 2017. Aedes aegypti Piwi4 is a non-canonical PIWI protein involved in antiviral responses. mSphere 2 e00144-00117.
Verhulst, E.C., van de Zande, L., 2015. Double nexus–Doublesex is the connecting element in sex determination. Brief Funct Genomics 14, 396–406.
Wise de Valdez, M.R., Nimmo, D., Betz, J., Gong, H.F., James, A.A., Alphey, L., Black, W.C.t., 2011. Genetic elimination of dengue vector mosquitoes. In: Proceedings of the National Academy of Sciences of the United States of America. 108. pp. 4772–4775.
Yoshimi, K., Kunihiro, Y., Kaneko, T., Nagahora, H., Voigt, B., Mashimo, T., 2016. ssODN-mediated knock-in with CRISPR-Cas for large genomic regions in zygotes. Nat. Commun. 7, 10431.